

# Mesoporous Aluminophosphate Molecular Sieves Synthesized under Nonaqueous Conditions<sup>†</sup>

Michael Tiemann,<sup>‡</sup> Marcus Schulz,<sup>§</sup> Christian Jäger,<sup>§</sup> and Michael Fröba<sup>\*,‡,||</sup>

*Institute of Inorganic and Applied Chemistry, University of Hamburg, Martin-Luther-King-Platz 6, D-20146 Hamburg, Germany, Institute of Optics and Quantum Electronics, Friedrich-Schiller-University, Max-Wien-Platz 1, D-07743 Jena, Germany, and Institute of Inorganic and Analytical Chemistry, Justus-Liebig-University Giessen, Heinrich-Buff-Ring 58, D-35392 Giessen, Germany*

Received February 7, 2001

Long-chain *n*-alkylamine surfactants have been used as structure-directing agents in the synthesis of mesoporous aluminophosphates by a highly cooperative formation mechanism in an alcoholic system. Small amounts of water in the synthesis mixture play a significant role in the hydrolysis of the aluminum precursor (Al[O<sup>+</sup>Pr]<sub>3</sub>) and are important for the quality of the mesostructured products. The materials exhibit disordered mesostructures, the stability and structural order of which can be improved by a postsynthetic thermal treatment. The products are then stable enough for the removal of the surfactant molecules by acidic solvent extraction, yielding surface areas up to 690 m<sup>2</sup>/g.

## Introduction

The utilization of supramolecular assemblies of surfactants as structure-directing species for the preparation of mesostructured materials, as introduced in 1992 for silica and aluminosilicate phases,<sup>1</sup> has in recent years been applied to the synthesis of several mesostructured aluminophosphates. Many of these materials have lamellar or hexagonal structures that are thermally unstable and therefore collapse when the template is removed by calcination,<sup>2–10</sup> but some of the products exhibit mesopores in a hexagonal or disordered arrangement after the removal of the surfactant.<sup>11–16</sup>

For most of these materials, especially for the thermally stable porous phases, structure direction was achieved by the utilization of long-chain cationic *n*-alkyl trimethylammonium surfactants.<sup>9–12,14,15</sup> In other cases neutral *n*-alkylamines were employed, leading to lamellar mesostructures or to microporous hexagonal materials, respectively.<sup>2–6,16</sup> Mesoporous phases were also obtained from a synthesis using anionic sodium dodecyl sulfate.<sup>13</sup> Finally, alkylphosphate surfactants have been used for the syntheses of various mesostructured aluminophosphates.<sup>7,8</sup>

The majority of the syntheses mentioned above was carried out in aqueous systems. However, in some cases unbranched primary alcohols and/or tetraethylene glycol were combined with small quantities of water.<sup>3,5,8,10b</sup> The same is true for the synthesis of mesoporous aluminum oxides under alcoholic conditions utilizing nonionic<sup>17</sup> or

\* To whom correspondence should be addressed. E-mail: Michael.Froeba@anorg.chemie.uni-giessen.de.

<sup>†</sup> This work is dedicated to Prof. Wolfgang Metz on the occasion of his 65th birthday.

<sup>‡</sup> University of Hamburg.

<sup>§</sup> Friedrich-Schiller-University.

<sup>||</sup> Justus-Liebig-University Giessen.

(1) (a) Kresge, C. T.; Leonowicz, M. E.; Roth, W. J.; Vartuli, J. C.; Beck, J. S. *Nature* **1992**, *359*, 710–712. (b) Beck, J. S.; Vartuli, J. C.; Roth, W. J.; Leonowicz, M. E.; Kresge, C. T.; Schmitt, K. D.; Chu, C. T.-W.; Olson, D. H.; Sheppard, E. W.; McCullen, S. B.; Higgins, J. B.; Schlenker, J. L. *J. Am. Chem. Soc.* **1992**, *114*, 10834–10843.

(2) Kraushaar-Czarnetzki, B.; Stork, W. H. J.; Dogterom, R. J. *Inorg. Chem.* **1993**, *32*, 5029–5033.

(3) Oliver, S.; Coombs, N.; Ozin, G. A. *Adv. Mater.* **1995**, *7*, 931–935. (b) Oliver, S.; Kuperman, A.; Coombs, N.; Lough, A.; Ozin, G. A. *Nature* **1995**, *378*, 47–50. (c) Ozin, G. A.; Oliver, S. *Adv. Mater.* **1995**, *7*, 943–947.

(4) (a) Sayari, A.; Karra, V. R.; Reddy, J. S.; Moudrakovski, I. L. *Chem. Commun.* **1996**, 411–412. (b) Chenite, A.; Le Page, Y.; Karra, V. R.; Sayari, A. *Chem. Commun.* **1996**, 413–414. (c) Sayari, A.; Moudrakovski, I.; Reddy, J. S.; Ratcliffe, C. I.; Ripmeester, J. A.; Preston, K. F. *Chem. Mater.* **1996**, *8*, 2080–2088.

(5) (a) Gao, Q.; Xu, R.; Chen, J.; Li, R.; Li, S.; Qui, S.; Yue, Y. *J. Chem. Soc., Dalton Trans.* **1996**, 3303–3307. (b) Gao, Q.; Chen, J.; Xu, R.; Yue, Y. *Chem. Mater.* **1997**, *9*, 457–462.

(6) Cheng, S.; Tzeng, J.-N.; Hsu, B.-Y. *Chem. Mater.* **1997**, *9*, 1788–1796.

(7) (a) Fröba, M.; Tiemann, M. *Chem. Mater.* **1998**, *10*, 3475–3483. (b) Schulz, M.; Tiemann, M.; Fröba, M.; Jäger, C. *J. Phys. Chem. B* **2000**, *104*, 10473–10481.

(8) (a) Tiemann, M.; Fröba, M.; Rapp, G.; Funari, S. S. *Chem. Mater.* **2000**, *12*, 1342–1348. (b) Tiemann, M.; Fröba, M.; Rapp, G.; Funari, S. S. *Stud. Surf. Sci. Catal.* **2000**, *129*, 559–566.

(9) (a) Khimyak, Y. Z.; Klinowski, J. *Chem. Mater.* **1998**, *10*, 2258–2265. (b) Khimyak, Y. Z.; Klinowski, J. *J. Chem. Soc., Faraday Trans.* **1998**, *94*, 2241–2247.

(10) (a) Feng, P.; Xia, Y.; Feng, J.; Bu, X.; Stucky, G. D. *Chem. Commun.* **1997**, 949–950. (b) Feng, P.; Bu, X.; Stucky, G. D. *Inorg. Chem.* **2000**, *39*, 2–3.

(11) (a) Zhao, D.; Luan, Z.; Kevan, L. *Chem. Commun.* **1997**, 1009–1010. (b) Zhao, D.; Luan, Z.; Kevan, L. *J. Phys. Chem. B* **1997**, *101*, 6943–6948. (c) Luan, Z.; Zhao, D.; He, H.; Klinowski, J.; Kevan, L. *J. Phys. Chem. B* **1998**, *102*, 1250–1259.

(12) (a) Kimura, T.; Sugahara, Y.; Kuroda, K. *Chem. Commun.* **1998**, 559–560. (b) Kimura, T.; Sugahara, Y.; Kuroda, K. *Microporous Mesoporous Mater.* **1998**, *22*, 115–126. (c) Kimura, T.; Sugahara, Y.; Kuroda, K. *Chem. Mater.* **1999**, *11*, 508–518.

(13) (a) Holland, B. T.; Isbester, P. K.; Blanford, C. F.; Munson, E. J.; Stein, A. *J. Am. Chem. Soc.* **1997**, *119*, 6796–6803. (b) Holland, B. T.; Isbester, P. K.; Munson, E. J.; Stein, A. *Mater. Res. Bull.* **1999**, *34*, 471–482. (c) Kron, D. A.; Holland, B. T.; Wipson, R.; Maleke, C.; Stein, A. *Langmuir* **1999**, *15*, 8300–8308.

(14) (a) Chakraborty, B.; Pulikottil, A. C.; Das, S.; Viswanathan, B. *Chem. Commun.* **1997**, 911–912. (b) Chakraborty, B.; Pulikottil, A. C.; Viswanathan, B. *Appl. Catal. A* **1998**, *167*, 173–181.

(15) Cabrera, S.; Haskouri, J. E.; Guillem, C.; Beltrán-Porter, A.; Beltrán-Porter, D.; Mendioroz, S.; Marcos, M. D.; Amorós, P. *Chem. Commun.* **1999**, 333–334.

(16) Eswaramoorthy, M.; Neeraj, S.; Rao, C. N. R. *Microporous Mesoporous Mater.* **1999**, *28*, 205–210.

anionic amphiphiles,<sup>18</sup> respectively. All nonaqueous syntheses of aluminophosphates reported so far did not lead to mesoporous materials. The literature on mesostructured aluminophosphates synthesized with the utilization of supramolecular structure directors has recently been reviewed.<sup>19</sup>

Here, we report on the first synthesis of mesoporous aluminophosphates under basically nonaqueous conditions with low quantities of water present in the reaction mixture; this is also the first time that the utilization of primary *n*-alkylamine surfactants leads to porous mesostructured aluminophosphate materials.

### Experimental Section

**Synthesis.** In a typical synthesis 8.2 g Al(O<sup>+</sup>Pr)<sub>3</sub> (Merck) is added to a solution of 4.6 g of H<sub>3</sub>PO<sub>4</sub> (85%, Merck) in 50 g of ethanol (99.8%) and 1.4 g of water. (The relative amount of water was varied as discussed below.) The mixture is stirred vigorously for 30 min at room temperature. A solution of 4.8 g of C<sub>16</sub>H<sub>33</sub>NH<sub>2</sub> (Merck) in 10 g of ethanol (99.8%) is then added (corresponding to an approximate molar ratio in the synthesis mixture of Al/P/surfactant/ethanol/water = 1/1/0.5/32/3). After being stirred at room temperature for another 30 min, the slurry is transferred into a Teflon-lined autoclave and kept at 90 °C for 48 h without agitation. The product is filtered off, washed with ethanol, and dried.

**Postsynthetic Treatment.** In a postsynthetic treatment 5 g of the dry sample is stored in a closed container over 10 g of water. The container is sealed and stored at 90 °C for 12 h without agitation. By this procedure the sample is exposed to water vapor, but is not in contact with liquid water.

**Surfactant Extraction.** For the extraction of the surfactant 5 g of the sample (after the postsynthetic treatment) is dispersed in a solution of 20 g of methanol and 5 g of aqueous hydrochloric acid (1 mol/l). The mixture is stirred at room temperature for 15 min, filtered off, and washed with methanol. The process is repeated three times.

**Characterization.** Powder X-ray diffraction patterns were recorded on a Bruker AXS D8 Advance diffractometer (Cu K $\alpha$  radiation) equipped with a secondary monochromator. Transmission electron microscopic (TEM) images were taken on a Philips STEM 400 electron microscope. Simultaneous thermogravimetry, differential thermal analysis, and mass spectrometry (TG/DTA/MS) was performed on a Netzsch STA 409 thermobalance coupled with a Baltzer QMG 421 quadrupole mass spectrometer (multiple ion detection method). Physisorption analysis was carried out on a Quantachrome Autosorb 1 apparatus; the samples were dried at 90 °C in high vacuum for 12 h. Specific surface areas were calculated by the BET equation for relative pressures between 0.05 and 0.2; pore size distributions were calculated by the BJH formula from the desorption isotherm. Infrared (IR) spectroscopic measurements were performed in a KBr matrix on a Perkin-Elmer FT-IR 1720 spectrometer.

Solid-state <sup>27</sup>Al and <sup>31</sup>P MAS NMR spectroscopy was carried out on a Bruker ASX 400 spectrometer operating at a magnetic field of B<sub>0</sub> = 9.4 T with NMR frequencies of 102 MHz for <sup>27</sup>Al and 161 MHz for <sup>31</sup>P NMR, respectively. The rotation frequency was 10 kHz. The <sup>27</sup>Al triple quantum MAS experiment (MQMAS)<sup>20–22</sup> was carried out using the z-filter sequence with three rf pulses at a rotation frequency of 10 kHz. Pulse widths of 3.6 and 1.8  $\mu$ s for the first two pulses were used at a B<sub>1</sub>

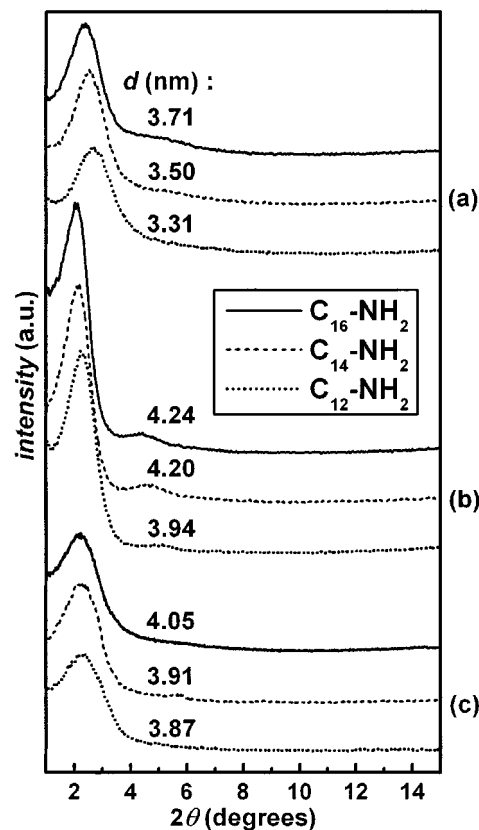


**Figure 1.** Powder XRD patterns of mesostructured aluminophosphates prepared with C<sub>12</sub>-NH<sub>2</sub>, C<sub>14</sub>-NH<sub>2</sub>, and C<sub>16</sub>-NH<sub>2</sub>: (a) as-synthesized; (b) after thermal treatment; (c) after extraction of the surfactant. The patterns are typical of disordered tubular mesostructures. The structural order increases after thermal treatment and remains intact after surfactant removal.

field strength that corresponds to 100 kHz. The third weak pulse was 8- $\mu$ s long at a B<sub>1</sub> field strength of 20 kHz. A total of 128 t<sub>1</sub> increments (15- $\mu$ s incrementation time, hypercomplex data acquisition) were measured, corresponding to a sweep width of the f<sub>1</sub> triple quantum dimension of 66.7 kHz. Each slice was measured with 480 scans.

X-ray absorption (XANES) spectra at the Al K-edge were recorded at beamline SA32 at the Laboratoire pour l'Utilisation du Rayonnement Électromagnétique (LURE), Centre Universitaire Paris-Sud, Orsay Cedex, France, using a quartz double-crystal monochromator. Measurements were carried out at room temperature in total electron yield mode; the electron storage ring was running at 0.8 GeV with currents of ca. 220–420 mA. The spectra were calibrated against the edge position of pure aluminum (1559 eV), pre-edge fitted, and normalized with WINXAS software.<sup>23</sup>

### Results and Discussion

**Synthesis.** The utilization of long-chain primary alkylamines as structure-directing agents under alcoholic conditions leads to aluminophosphates with disordered mesostructures. Figure 1a shows the X-ray diffraction (XRD) patterns of the *as-synthesized* products prepared with C<sub>12</sub>-NH<sub>2</sub>, C<sub>14</sub>-NH<sub>2</sub>, and C<sub>16</sub>-NH<sub>2</sub>, respectively. Each pattern consists of one relatively broad reflection at low diffraction angle. This is a typical indication of a randomly ordered arrangement of rodlike surfactant arrays within the inorganic matrix; similar

(17) Bagshaw, S. A.; Pinnavaia, T. J. *Angew. Chem., Int. Ed. Engl.* **1996**, *35*, 1102–1105.

(18) Vaudry, F. J.; Khodabandeh, S.; Davis, M. E. *Chem. Mater.* **1996**, *8*, 1451–1464.

(19) Tiemann, M.; Fröba, M. *Chem. Mater.* **2001**, in press.

(20) Frydman, L.; Harwood, S. J. *J. Am. Chem. Soc.* **1995**, *117*, 5367–5368.

(21) Amoureux, J. P. *Solid State NMR* **1996**, *6*, 73–83.

(22) Massiot, A.-R.; Kretschner, A.; Cajipe, V. C. *Magn. Reson. Chem.* **1997**, *35*, 86.

(23) Ressler, T. J. *Synchrotron Radiat.* **1998**, *5*, 118–122.

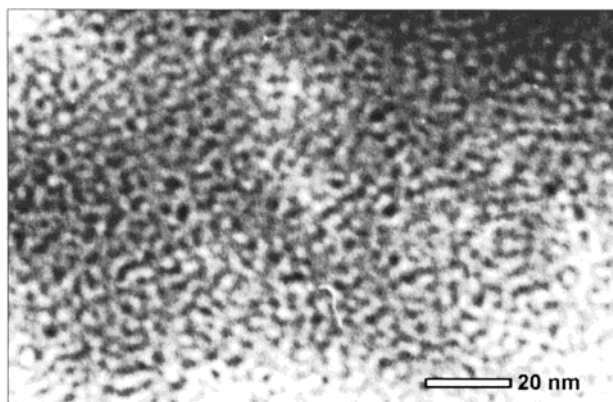


**Figure 2.** Representative transmission electron micrograph (TEM) of a mesostructured aluminophosphate prepared with  $C_{16}\text{-NH}_2$  showing a disordered mesostructure on the scale of several nanometers.

**Table 1. Molar Compositions of Three Representative Mesostructured Aluminophosphate Samples (As-Synthesized) According to Elemental Analysis**

surfactant	elemental analysis				Al/P	$C_n\text{-NH}_2/\text{P}$
	Al	P	C	N		
$C_{12}\text{-NH}_2$	0.140	0.125	0.682	0.053	1.12	0.45
$C_{14}\text{-NH}_2$	0.117	0.102	0.730	0.050	1.14	0.51
$C_{16}\text{-NH}_2$	0.122	0.108	0.723	0.044	1.14	0.42

structures have often been observed among various mesostructured materials,<sup>24</sup> including aluminophosphates.<sup>11,15</sup> Depending on the chain lengths of the surfactants, the three products exhibit different  $d$ -spacings corresponding to different XRD diffraction angles. Figure 2 shows a representative transmission electron micrograph (TEM) of an *as-synthesized* sample prepared with  $C_{16}\text{-NH}_2$ , in which the disordered mesostructure is evident.

Table 1 shows the elemental analysis of the three *as-synthesized* samples described above. The Al/P ratios in the products are between 1.12 and 1.14, which indicates that the samples may basically be regarded as aluminophosphates rather than consisting, to a significant degree, of aluminum oxide species; the latter would certainly lead to a lower relative amount of phosphorus. This is confirmed by NMR data (see below). Elemental analysis also shows that the molar  $C_n\text{-NH}_2/\text{P}$  ratio is between 0.42 and 0.51 (corresponding to a  $C_n\text{-NH}_2/\text{Al}$  ratio between 0.37 and 0.45), which means that not all the surfactant used for the synthesis (0.5 mol  $C_n\text{-NH}_2$  per  $\text{H}_3\text{PO}_4$ ) is found in the products.

As described in the Experimental Section, the reaction mixtures are not completely free of water during the syntheses; the approximate molar ratio of Al/water is 1/3. Water turns out to be essential for the successful preparation of well-ordered mesostructures. When lower amounts of water are used, the quality of the products becomes somewhat poorer, that is, the samples display weaker X-ray diffractions and are thermally less stable. Higher amounts of water, on the other hand, lead to the formation of a second mesophase with a lamellar structure, comparable to those obtained from syntheses carried out entirely in water.<sup>4</sup> The influence of water on the quality of the products will be further discussed

in the context of postsynthetic thermal treatment of the samples (see below).

The alkylamine surfactants used are completely soluble in ethanol under the conditions used in the syntheses. The pure surfactant solutions are optically isotropic at room temperature as well as at 90 °C, as was verified by polarized-light optical microscopy and small-angle X-ray scattering (SAXS, experimental details provided elsewhere<sup>8</sup>). Hence, the evolution of a mesostructure during the synthesis is obviously induced by the presence of the inorganic reactants; the formation of the mesostructure is a highly cooperative process.

Attempts to remove the surfactant from the *as-synthesized* products without collapse of the mesostructure were not successful. Before the postsynthetic thermal treatment (see below), calcination of the samples results in the complete disappearance of the X-ray reflections and no significant specific surface area is found by physisorption measurements. Similarly, solvent extraction under the conditions necessary for a quantitative removal of the surfactant (i.e., acidic methanol extraction at room temperature, see below) leads to a significant decrease in structural order and to low specific surface areas of 100–300  $\text{m}^2/\text{g}$ .

**Postsynthetic Treatment and Surfactant Removal.** It is possible to improve the stability of the samples as well as the degree of structural order by postsynthetic thermal treatment in an atmosphere of water vapor. In this procedure the samples are exposed to water vapor at 90 °C, but are not in contact with liquid water. In contrast, thermal treatment of the samples dispersed in liquid water leads to a phase transition into lamellar mesostructures. On the other hand, storage of the dry samples at 90 °C without water vapor does not result in any improvement of the stability or structural order; hence, the presence of water plays an essential role in the thermal treatment. Figure 1b shows the powder XRD patterns of the thermally treated samples. The intensity of the reflection has increased and is shifted to a lower diffraction angle corresponding to a larger  $d$ -spacing as compared to the that of the *as-synthesized* product. According to elemental analysis, the relative Al/P/ $C_n\text{-NH}_2$  ratios do not change significantly in the course of the thermal treatment.

The relatively poor stability of the *as-synthesized* products indicates an incomplete condensation of  $\text{PO}_4$  units with aluminum atoms which, in turn, are most likely coordinated by additional water and/or hydroxyl groups to give the tetrahedral and octahedral aluminum environment observed (see below). Such an incompletely condensed framework with  $\text{Al}(\text{OP})_{4-x}(\text{H}_2\text{O})_x$  has been reported.<sup>12</sup> In light of this assumption, the postsynthetic thermal treatment obviously leads to an additional, i.e., more complete, framework condensation by which the stability as well as the structural order are improved.

Another possible interpretation of the effects of the thermal treatment is that the hydrolysis of the aluminum precursor,  $\text{Al}(\text{O}^i\text{Pr})_3$ , which proceeds slower in alcohols than in water, is not completed after the initial synthesis and that a further hydrolysis takes place during the postsynthetic treatment. However, according to elemental analysis, the N/C ratios in the *as-synthesized* products correspond to those of the re-

(24) (a) Tanev, P. T.; Pinnavaia, T. J. *Science* **1995**, *267*, 865–867. (b) Tanev, P. T.; Pinnavaia, T. J. *Chem. Mater.* **1996**, *8*, 2068–2079.



spective surfactants (i.e., 1/12 for C<sub>12</sub>-NH<sub>2</sub>, 1/14 for C<sub>14</sub>-NH<sub>2</sub>, and 1/16 for C<sub>16</sub>-NH<sub>2</sub>). This indicates that the hydrolysis of the aluminum precursor, Al(O<sup>i</sup>Pr)<sub>3</sub>, is already completed before the postsynthetic thermal treatment; otherwise, additional amounts of carbon would be found due to remaining isopropoxide ligands attached to aluminum. The C/N ratio does not change significantly after the thermal treatment. Thus, the role of the water in the postsynthetic treatment is not to be attributed to a further, i.e., more complete, hydrolysis of the aluminum reactant.

The increase in the *d*-spacing in the course of the thermal treatment may, on one hand, be explained by a growth of the inorganic walls due to the additional condensation of the inorganic units. On the other hand, the rodlike domains between the inorganic walls, where the surfactant molecules reside, may expand. As pointed out above, water is essential in the postsynthetic thermal process; to reach all parts of the inorganic domains, the water molecules may well be envisioned to be transported through the rodlike channel system by diffusion (most likely along the boundary regions between the surfactant headgroups and the inorganic part), by which they could cause a swelling of the channel diameter.

After the postsynthetic thermal treatment the materials are stable enough to preserve their mesostructure upon removal of the surfactant by acidic extraction with methanol. For a quantitative extraction it has turned out necessary to use at least equimolar amounts of HCl with respect to the approximate amount of surfactant to be extracted. This indicates a cation exchange mechanism during the extraction in which the surfactant molecules, with their headgroups protonated (i.e., R-NH<sub>3</sub><sup>+</sup>), are replaced by protons. After extraction the samples still exhibit the characteristic, though broader and slightly less intense, low-angle XRD reflections; the *d*-spacings are slightly lower than those before the extraction, which is not unusual (Figure 1c).

The complete removal of the surfactant is confirmed by the fact that no carbon is found by elemental analysis in the samples after extraction. Also, infrared (IR) spectroscopy shows that the characteristic C-H valence bands at 2930–2850 cm<sup>-1</sup> as well as C-H deformation bands around 1460 and 720 cm<sup>-1</sup> are absent after extraction (Figure 3). The surfactant can be isolated from the neutralized solution of the extract. After the removal of the surfactant, the samples are thermally stable at temperatures up to ca. 500 °C.

The porous nature of the materials after the extraction of the template was investigated by physisorption measurements. Figure 4 shows the nitrogen adsorption/desorption isotherm of the sample prepared with C<sub>16</sub>-NH<sub>2</sub>. At a relative pressure between 0.35 and 0.45, a well-defined step occurs, indicating capillary condensation. The isotherm is of type IV,<sup>25</sup> as typical of mesoporous materials; the specific surface area is 690 m<sup>2</sup>/g. The pore size distribution (diameter) has its maximum at 3.33 nm (Figure 5). Corresponding results are found for products prepared with C<sub>12</sub>-NH<sub>2</sub> or C<sub>14</sub>-NH<sub>2</sub>, respectively.

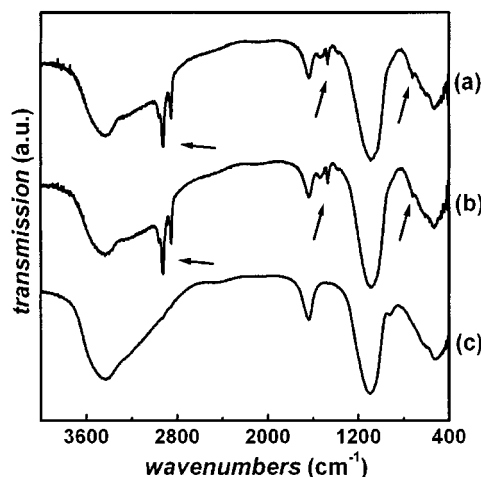


**Figure 3.** IR spectra of mesostructured aluminophosphates prepared with C<sub>16</sub>-NH<sub>2</sub>: (a) as-synthesized; (b) after thermal treatment; (c) after extraction of the surfactant. The arrows indicate characteristic C-H bands in the surfactant hydrocarbon chain, which disappear after its removal.

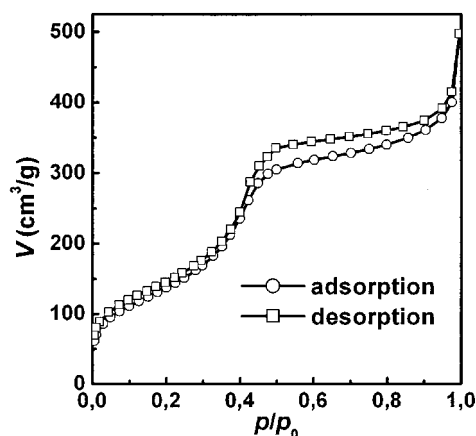


**Figure 4.** Nitrogen adsorption/desorption isotherm of a mesoporous aluminophosphate prepared with C<sub>16</sub>-NH<sub>2</sub>; the specific BET surface area is 690 m<sup>2</sup>/g. An increase in the slope of both isotherm branches at ca.  $p/p_0 = 0.35-0.45$  indicates mesoporosity.

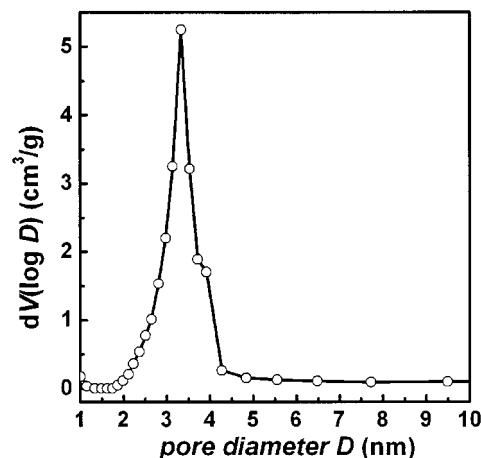


**Figure 5.** BJH pore size distribution (diameter) as calculated from the desorption branch in Figure 4.

The sorption isotherms show a hysteresis parallel to the pressure axis above the relative pressure at which capillary condensation occurs; this may be explained by physisorption in the interparticle pore system: During

(25) Sing, K. S. W.; Everett, D. H.; Haul, R. A. W.; Moscou, L.; Pierotti, R. A.; Rouqu rol, J.; Siemieniwska, T. *Pure Appl. Chem.* **1985**, *57*, 603–619.

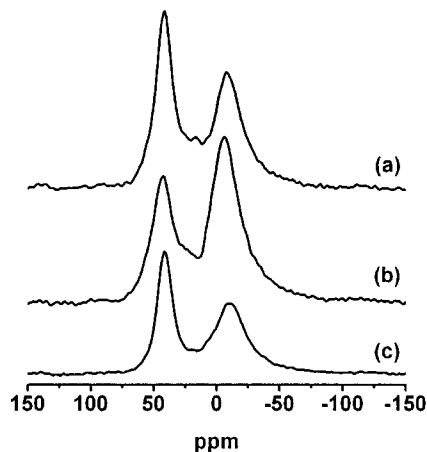


**Figure 6.** Solid-state MAS  $^{27}\text{Al}$  NMR spectra of mesostructured aluminophosphates prepared with  $\text{C}_{16}\text{-NH}_2$ : (a) as-synthesized; (b) after thermal treatment; (c) after surfactant extraction. The spectra show two resonances at ca. 42 and  $-7$  ppm corresponding to  $\text{Al}(\text{OP})_4$  and  $\text{Al}(\text{OP})_x(\text{H}_2\text{O})_{6-x}$ , respectively; a weakly resolved third resonance at ca. 20 ppm can be suspected (cf. Figure 7).

the desorption, nitrogen in the supercritical state remains adsorbed on the interparticle surface; the (supposedly) small and uniform particle sizes lead to small distances between adjacent particles that are roughly in the same order of magnitude as the diameter of the tubular mesopores. This is consistent with the occurrence of a weak shoulder in the pore size distribution calculated from the desorption isotherm (BJH) at ca. 4 nm (diameter); the shoulder is absent if the pore size distribution is calculated from the adsorption branch. This hysteresis effect has been observed before.<sup>26–28</sup> A closing of the hysteresis at a relative pressure of  $p/p_0 = 0.42$  is to be expected; however, in the case studied here, this value coincides with the capillary condensation step in both isotherms (adsorption and desorption), which means that the reversibility cannot be verified.

The extraction of the surfactant with methanol under acidic conditions is a very mild and convenient method for the complete removal of the organic template from the samples. Moreover, the surfactant can be rescued and reused after the extraction, which offers an economic advantage.

**Further Characterization of the Products.** To obtain information on the short-range coordination environment of aluminum, the samples were investigated by  $^{27}\text{Al}$  MAS NMR spectroscopy; Figure 6 shows the spectra of a sample prepared with  $\text{C}_{16}\text{-NH}_2$  before and after thermal treatment as well as after surfactant extraction. All three spectra exhibit a resonance at ca. 42 ppm, which corresponds to tetrahedral  $\text{Al}(\text{OP})_4$  groups, and another resonance at ca.  $-7$  ppm, which is attributable to 6-fold coordinated Al with P in the second coordination shell and, presumably, additional  $\text{H}_2\text{O}$  or OH groups, i.e.,  $\text{Al}(\text{OP})_x(\text{H}_2\text{O})_{6-x}$ .<sup>7</sup> Additionally, there is a weakly resolved resonance around 20 ppm which can be identified unambiguously only in the MQMAS spectrum shown in Figure 7; this signal can be attributed to 5-fold coordinated Al, again with P in the second shell,

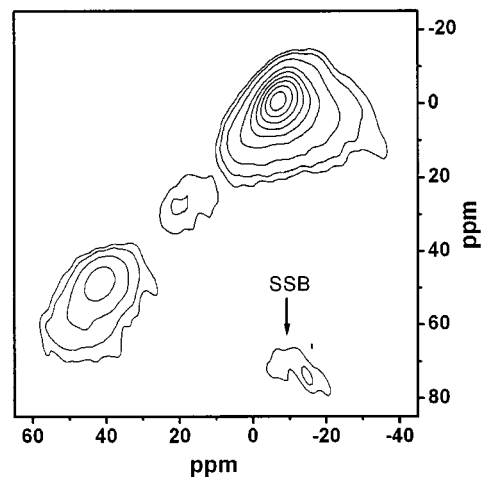


**Figure 7.** Sheared  $^{27}\text{Al}$  MQMAS spectrum of a mesostructured aluminophosphate (as-synthesized) prepared with  $\text{C}_{16}\text{-NH}_2$ . Apart from the two signals at ca. 42 and  $-7$  ppm, the spectrum resolves a third resonance at ca. 20 ppm, which cannot be identified unambiguously in the MAS spectrum (cf. Figure 6) and may be attributed to coordinated  $\text{Al}(\text{OP})_x(\text{H}_2\text{O})_{5-x}$  (SSB: spinning sideband.)

i.e.,  $\text{Al}(\text{OP})_x(\text{H}_2\text{O})_{5-x}$ . The NMR spectra do not indicate the presence of any significant amounts of aluminum oxide and/or oxyhydroxide species in the samples. An interesting observation is that in the MAS spectra the relative intensity of the resonance at  $-10$  ppm (i.e., the relative amount of octahedrally coordinated Al) considerably increases after the thermal treatment, which indicates that during this treatment (which is carried out under a water atmosphere) additional water molecules coordinate to previously tetrahedral Al sites. This process seems to be reversible since after the extraction of the surfactant (under nonaqueous conditions) the relative amount of tetrahedral Al returns to approximately its original value. In summary, the NMR data strongly suggest that the inorganic part of the samples consists of an aluminophosphate network with Al–O–P linkages.

The  $^{31}\text{P}$  MAS NMR spectra of the same samples prepared with  $\text{C}_{16}\text{-NH}_2$  (before and after thermal treatment as well as after surfactant extraction) are shown in Figure 8. They exhibit relatively broad signals between 0 and  $-30$  ppm. In the case of the samples before the surfactant extraction (a and b), the signals seem to consist of several resonances which are badly resolved from each other. These resonances may be attributed to 4-fold coordinated P with O–Al (tetrahedral and/or octahedral Al) and various amounts of  $\text{H}_2\text{O}$  or OH groups, i.e.,  $\text{P}(\text{OAl})_x(\text{H}_2\text{O})_{4-x}$ . Very similar  $^{31}\text{P}$  MAS NMR spectra were reported by Sayari et al. for lamellar mesostructured aluminophosphate synthesized under aqueous conditions with the utilization of the same primary amine surfactants.<sup>4</sup> However, the bad resolution of these resonances does not allow for more specific assignments to the diverse P environments. Particularly, it is not possible to distinguish between the P environment in the *as-synthesized* sample (a) and in the thermally treated sample (b). Finally, the spectrum of the extracted sample (c) shows a similarly broad signal which exhibits a more symmetric shape than that of the samples before extraction; it is not possible to distinguish whether it consists of one or more than one

(26) Sonwane, C. G.; Bhatia, S. K. *Langmuir* **1999**, *15*, 2809–2816.

(27) Long, Y.; Xu, T.; Sun, Y.; Dong, W. *Langmuir* **1998**, *14*, 6173–6178.

(28) Köhn, R.; Thommes, M., private communication.

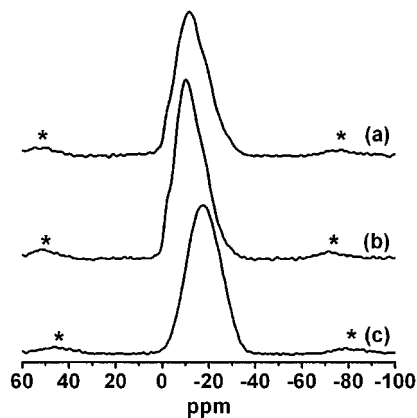


**Figure 8.** Solid-state MAS  $^{31}\text{P}$  NMR spectra of mesostructured aluminophosphates prepared with  $\text{C}_{16}\text{-NH}_2$ : (a) as-synthesized; (b) after thermal treatment; (c) after surfactant extraction. The spectra show broad lines which may consist of several resonances corresponding to  $\text{P}(\text{OAl})_x(\text{H}_2\text{O})_{4-x}$ . The asterisks indicate spinning sidebands.

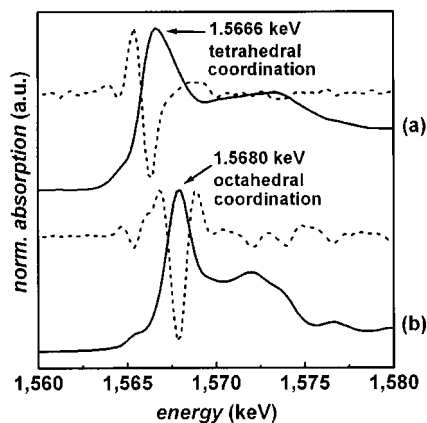


**Figure 9.** Al K-edge XANES spectra of (a) crystalline  $\text{AlPO}_4$  (*berlinite*) and (b)  $\alpha\text{-Al}_2\text{O}_3$  (*corundum*), serving as references for the distinction between tetrahedral and octahedral Al coordination, respectively. Solid lines, original spectra; dashed lines, second derivatives.

resonance. The signals are slightly shifted to lower fields as long as the surfactant molecules are still present (i.e., before the extraction); this may be explained by the influence of acidic protons of the surfactant headgroups ( $\text{R-NH}_3^+$ ).

Another convenient method to distinguish between tetrahedrally and octahedrally coordinated aluminum is provided by XANES spectroscopy at the Al K-edge; the exact energy position of the absorption maximum (corresponding to the 1s to 3p electronic transition) differs by approximately 1.5 eV for 4-fold (1.5666 keV) and 6-fold coordination (1.5680 keV), respectively. When both coordination numbers are present in the same sample, the two absorption maxima usually strongly overlap and may therefore be more conveniently distinguished in the second derivative of the spectrum, which shows two well-resolved minima at the respective energies.<sup>7a</sup> Figure 9 shows the spectra of two reference samples for tetrahedral and octahedral aluminum, respectively, as well as their second derivatives.

Figure 10 shows the Al K-edge XANES spectra (and second derivatives) of a sample prepared with  $\text{C}_{16}\text{-NH}_2$  before and after thermal treatment as well as after extraction of the surfactant; the spectra qualitatively

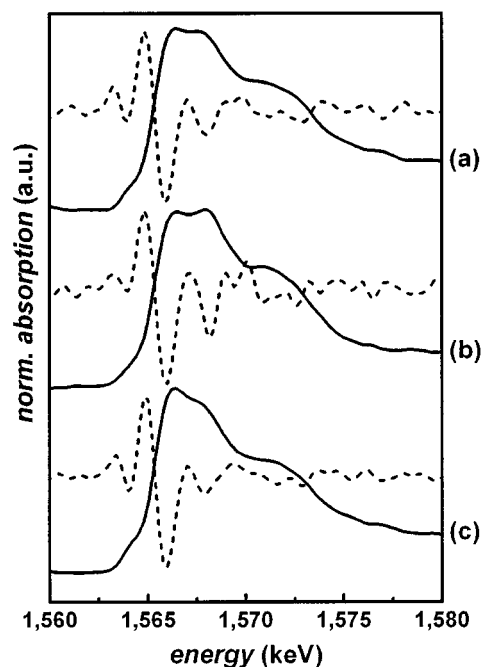


**Figure 10.** Al K-edge XANES spectra of mesostructured aluminophosphates prepared with  $\text{C}_{16}\text{-NH}_2$ : (a) as-synthesized; (b) after thermal treatment; (c) after surfactant extraction. Solid lines, original spectra; dashed lines, second derivatives.

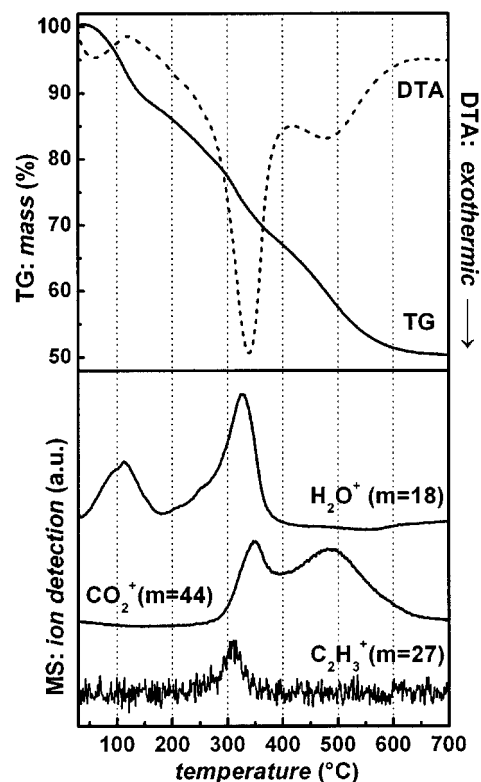


**Figure 11.** Simultaneous thermogravimetry (TG), differential thermal analysis (DTA), and mass spectrometry (MS) of a mesostructured aluminophosphate prepared with  $\text{C}_{16}\text{-NH}_2$ .

confirm the NMR data. However, a lower relative amount of octahedral Al, especially in the thermally treated sample, is found. Quantitative results derived from the XANES spectra may be less reliable than those from NMR data. On the other hand, it should be mentioned that different quantitative results were found

by both NMR and XANES, depending on the age of the samples; after several months an irreversible uptake of water from air (i.e., a higher relative amount of octahedral Al) was observed by both methods. Furthermore, dissimilar experimental conditions are used in XANES spectroscopy as compared to those in MAS NMR spectroscopy; for a XANES spectrum the sample is exposed to a high-intensity X-ray beam under vacuum, which may have some influence on the amount of water coordinated to Al.

Figure 11 shows the thermal analysis of an *as-synthesized* sample prepared with  $C_{16}-NH_2$ . The thermogravimetric (TG) plot reveals a continuous mass loss of ca. 47% between room temperature and ca. 650 °C. Taking into account the combination of differential thermal analysis (DTA) and mass spectrometry (MS), this mass loss can be divided up into three steps: Below ca. 200 °C there is a loss of water (ca. 10%), which may be physisorbed on the interparticle surface of the sample and/or reside within the channels, i.e., at the intraparticle surface. In a second step, between ca. 200 and 400 °C, a mass loss of ca. 18% is observed, during which both water and several organic fragments ( $C_2H_3^+$  shown as an example) as well as carbon dioxide are detected. This exothermic step is attributable to the beginning decomposition of the surfactant. Finally, in a third step (ca. 400–650 °C) another exothermic mass loss of ca. 19% occurs which is accompanied by the detection of carbon dioxide, corresponding to a further decomposition of the organic part. These results are representative of all *as-synthesized* samples; likewise, all materials show

the same thermal behavior after the postsynthetic thermal treatment.

### Conclusions

For the first time mesoporous aluminophosphates were synthesized under basically nonaqueous conditions, although small amounts of water turn out to play a vital role in these syntheses. Also, a postsynthetic thermal treatment of the samples, in which water is involved as a necessary factor, leads to a significant improvement of the quality of the materials. The alcoholic preparation offers new perspectives for future syntheses. It has also led to the first successful utilization of long-chain alkylamines for the preparation of nonlamellar mesoporous aluminophosphates.

**Acknowledgment.** We would like to thank LURE for allocating beamtime, Dr. Anne-Marie Flank, Dr. Pierre Lagarde, and Dr. Rogerio Junqueira Prado (LURE) for their help with the XANES studies, and Dr. Matthias Thommes (Quantachrome Corporation, Odelzhausen, Germany) and Ralf Köhn (University of Hamburg) for their help with the interpretation of the physisorption data. Financial support by *Deutsche Forschungsgemeinschaft* (Fr1372/5–1) and *Fonds der Chemischen Industrie* as well as funding of the work at LURE by the European Community (Access to Research Infrastructure action of the Improving Human Potential Program) is gratefully acknowledged.

CM011044P